SPACE
SCIENCES
LABORATORY

AURORAL MICROPULSATION INSTABILITY

By F. V. Coroniti and C. F. Kennel

Technical Report on
NASA ~~Grant NSG 243 and~~ NGL 05-003-012

Space Sciences Laboratory Series 10, Issue 38

UNIVERSITY OF CALIFORNIA, BERKELEY

Space Sciences Laboratory
University of California
Berkeley, California 94720

AURORAL MICROPULSATION INSTABILITY

By

F. V. Coroniti
Department of Physics and Space Sciences Laboratory
University of California, Berkeley, and
Department of Physics, University of California, Los Angeles

and

C. F. Kennel
Department of Physics
University of California, Los Angeles

Technical Report on

NASA Grant ~~NSG 243 and~~ NGL 05-003-012

Space Sciences Laboratory Series 10, Issue 38

This work was supported in part by National Aeronautics and Space Administration Grant N~~sG 243 and~~ NGL 05-003-012, University of California, Berkeley; National Science Foundation Grant GP-6817, Office of Naval Research Grant NONR-4756(01), Atomic Energy Commission Contract AT(11-1)-34, Project 157, and National Aeronautics and Space Administration Contract NGR 05-007-116, University of California, Los Angeles; and NASA Contract AVCO-NASW-1400, AVCO Everett Research Laboratory, Everett, Massachusetts.

Auroral Micropulsation Instability

F. V. Coroniti* and C. F. Kennel

Physics Department, University of California, Los Angeles, California 90024

Abstract

In this paper we describe a drift instability of Alfven waves driven by the sharp electron thermal gradient at the inner edge of the electron plasma sheet. The analysis predicts a localized instability with wavelengths perpendicular to the magnetic field comparable with an ion cyclotron radius and parallel wavelengths comparable with the length of field lines. The fastest growing wave should have an ≈ 10 second period, consistent with observations of Pi 1 micropulsations observed during substorms.

---

* Also at Physics Department, and Space Science Laboratory, University of California, Berkeley, California.

1. Introduction

Intense low frequency micropulsations occur during magnetic storms and auroral substorms. Ground magnetometer observations (McPherron, et al., 1968) reveal a variety of oscillations, each with its own local time and spectral characteristics, whose complex morphology makes it unlikely that a single mechanism explain all the observations. We attempt to identify ≈ 10 second period magnetic micropulsations, which are morning side manifestations of substorms associated with modulations of energetic electron precipitation fluxes (Parks, et al., 1968a) with a particular drift instability of Alfven waves, driven by the strong electron thermal gradient at the inner edge of the electron plasma sheet (Vasyliunas, 1968a, b; Frank, 1968).

Except for the Pc-1 band, micropulsation frequencies are much smaller than the equatorial proton cyclotron frequency. Thus, except for Pc-1, only extremely high energy particles can be in cyclotron resonance, of which there are presumably too few to trigger an instability. We therefore rule out cyclotron resonance interactions and pitch angle anisotropy as a low frequency micropulsation source.

Multiplying the long wave periods by a characteristic propagation speed (such as the Alfven speed) suggests that at least one micropulsation spatial dimension should be roughly the length of the line of force. Yet the association of 5-40 second period micropulsations with precipitation pulsations (McPherron, et al., 1968) yields indirect evidence that micropulsations are localized transverse to the magnetic field. Due to our poor understanding of mode structure, propagation, and ionospheric coupling, ground magnetometer measurements do not fix reliably the size and location of micropulsation generation regions. Since electrons are guided by the magnetic field, electron precipitation pulsations give inherently better information than micropulsations, which cannot be guaranteed a priori to be so guided. Barcus and Rosenberg (1965), Barcus, et al., (1966), and Parks, et al., (1968a), found electron precipitation pulsations to be limited to 100-200 km regions in the ionosphere, which project onto the equatorial plane as several thousand kilometer regions, less by far than the length of auroral lines of force.

The large scale lengths parallel and small lengths transverse to the magnetic field direction, together with the low frequency, are consistent with drift waves. Furthermore, drift instabilities derive their energy from spatial gradients in the distribution of resonant particles. In straight magnetic fields, the important wave-particle interaction is Landau resonance (i.e., the particle parallel velocity $v_\parallel$ matches the parallel phase velocity $\omega/k_\parallel$); the analog of Landau resonance in mirror geometry is bounce resonance. Cyclotron resonances do not affect low frequency drift instabilities.

The steep inner edge of the electron plasma sheet (Vasyliunas, 1968a) is an obvious candidate for various drift instabilities. We search here for one which produces magnetic micropulsations between the ion and electron bounce frequencies. While magnetic fluctuations on the ground could originate from a rotating ionospheric line current driven by a purely electrostatic wave (Wilson, 1966), a simpler hypothesis is that micropulsations are magnetically polarized in deep space. We therefore generalize, for magnetospheric conditions, an analysis by Mikhailovsky and Rudakov (1963) of drift instabilities of Alfven waves. D'Angelo (1969) has also suggested drift instabilities are responsible for micropulsations.

Earlier, Swift (1967) analyzed an electrostatic drift instability without considering coupling to an oscillating magnetic field.

Section 2 elucidates when Alfven waves can have drift couplings to resonant particles, using physical arguments drawn from the two-fluid theory of low frequency waves in spatially homogeneous plasmas and a uniform magnetic field. In section 3, we derive a kinetic theory dispersion relation for drift waves in a spatially inhomogeneous plasma, assuming the magnetic field approximately uniform. While the techniques used are standard, many approximations are needed. These are discussed in 3.2, and the calculation described in 3.3. Those uninterested in calculational details may turn to section 4, where a simple dispersion relation, appropriate to the auroral electron boundary, is described. Here the range of unstable frequencies and wavelengths for Alfven waves in a strong temperature gradient is outlined. A comparison with observations in section 5 indicates that the present ideas are consistent with the observed spatial localization, magnetic polarization, and range of unstable frequencies and wavelengths of 10 second micropulsations. However, further theoretical work removing many of our simplifying assumptions is needed for truly definitive conclusions.

2. Motivation of Drift Approximation

2.1) Introduction

Information about changing plasma conditions propagates at various characteristic wave and particle speeds. For example, in single-fluid hydromagnetics, the relevant waves are the fast, intermediate, and slow waves (Kantrowitz and Petschek, 1966). In spatially inhomogeneous plasmas, particle drifts are additional physically significant propagation speeds. When the magnetic field strength B and the ion (+) or electron (-) pressure $P^{\pm}$ have spatial gradients, the corresponding drifts are

$$\underset{\sim}{v}_D^{\pm} = \frac{v_\perp^2}{\Omega_\pm} \frac{\underset{\sim}{B} \times \underset{\sim}{\nabla} B}{B^2} \quad ; \qquad \underset{\sim}{v}_P^{\pm} = \frac{P^{\pm}}{\Omega_\pm} \frac{\underset{\sim}{B} \times \underset{\sim}{\nabla} \ln P^{\pm}}{\rho^{\pm} B} \tag{2.1}$$

where $v_\perp$ is the particle's velocity component perpendicular to the magnetic field, $\rho^{\pm}$ is the ion or electron mass density, $\underset{\sim}{B}$ is the magnetic field, and $\Omega_\pm = \pm\, eB/M_\pm c$ is the ion or electron frequency. (e is the magnitude of the electronic charge in esu; c , the velocity of light; and $M_\pm$, the ion or electron mass. Henceforth, we will use Gaussian units.) $\underset{\sim}{v}_D^{\pm}$ is an actual guiding center drift, while $\underset{\sim}{v}_P^{\pm}$, the pressure drift, is not; $\underset{\sim}{v}_P^{+} - \underset{\sim}{v}_P^{-}$ is the macroscopic drift between electrons and ions providing the diamagnetic magnetic field gradients associated with pressure gradients. We eventually treat B to be approximately uniform; therefore we concentrate on $\underset{\sim}{v}_P^{\pm}$. Let us now estimate its order of magnitude:

$$v_p^{\pm} \simeq c_+ \frac{R_+}{L_p^{+}} \ , \qquad v_p^{-} \simeq \left[\frac{T^-}{M_+}\right]^{1/2} \frac{R_+}{L_p^{-}} \left[\frac{T^-}{T^+}\right]^{1/2} \tag{2.2}$$

where c_+ is the ion thermal speed, $R_+ = c_+/\Omega_+$, the thermal ion cyclotron radius, and $T^{\pm}$ the ion or electron temperature in energy units. $L_p^{\pm}$ is a logarithmic pressure scale length. Ordinarily $R_+/L_p^{\pm} \ll 1$, so that $v_p^{\pm}$ is much smaller than the particle thermal speeds.

For weak spatial inhomogeneities, the dispersion relation obtained from homogeneous plasma theory often describes wave properties well. One index of the importance of drift corrections to the dispersion relation is the ratio of $v_p^{\pm}$, which is perpendicular to the magnetic field, to the perpendicular phase velocity obtained from homogeneous theory. When $k_\perp v_p^{\pm}/\omega \simeq 1$, plasma inhomogeneity significantly modifies the wave propagation speeds and unstable growth rates. Since $v_p^{\pm}$ is small, only small perpendicular phase velocity waves have important drift corrections. We search for such waves in section 2.2.

2.2) Low Frequency Waves in the Two-Fluid Approximation.

By treating the ion and electron gases separately, the two-fluid description allows for the effects of the finite inertia of the individual particle species, which manifests itself in the inability of first ions and then electrons to produce rapid variations in plasma current. The two-fluid dispersion relation for the three wave modes with frequencies below the electron plasma frequency is (Braginskii, 1957; Stringer, 1963; Formisano and Kennel, 1969)

$$[c_F^{\,2} - (\omega^2/k^2)]\ [c_I^{\,2} - (\omega^2/k^2)]\ [c_{SL}^2 - (\omega^2/k^2)] =$$

$$= \frac{\omega^2}{k^2}\,[c_S^{\,2} - (\omega^2/k^2)]\ c_I^{\,2}\ \frac{k^2 c_A^{\,2}}{\Omega_+^{\,2}} \qquad (2.3)$$

where ω is the wave frequency, k the wave number, and ω/k the phase velocity. c_F, c_I, and c_{SL} are the fast, intermediate, and slow hydromagnetic wave speeds, defined by

$$\left.\begin{matrix} c_F{}^2 \\ \\ c_{SL}^2 \end{matrix}\right\} = \frac{c_A{}^2 + c_S{}^2}{2} \begin{matrix} + \\ \\ - \end{matrix} \left[\left(\frac{c_S{}^2 + c_A{}^2}{2} \right)^2 - c_S{}^2\, c_A{}^2 \cos^2\theta \right]^{1/2}$$

$$c_I{}^2 = c_A{}^2 \cos^2\theta \tag{2.4}$$

$\theta = \cos^{-1} k_{\parallel}/k$ is the angle between the wave vector and the magnetic field, c_A is the Alfven speed

$$c_A{}^2 = B_o{}^2/4\pi N M_+ \tag{2.5}$$

where N is the equilibrium number density, c_S , the sound speed

$$c_S{}^2 = \frac{\gamma_+ T^+ + \gamma_- T^-}{M_+} \tag{2.6}$$

and $\gamma_\pm$, the ion or electron ratio of specific heats.

The term $k^2 c_A{}^2/\Omega_+{}^2$ represents finite ion inertia. The current velocities in hydromagnetic waves are the order of c_A ; for wavelengths comparable with the ion cyclotron radius based upon c_A, ion currents decouple from the waves. Since ion inertia is decoupled from moving lines of force, the effective Alfven wave speed increases; since the degree of decoupling is wavelength dependent, the propagation is dispersive. When k increases to ω_{p_-}/c , finite electron inertia reduces the electron current, thereby slowing the effective Alfven speed. Since this occurs at wavelengths much shorter than those of interest here, finite electron inertia terms have been dropped in (2.2). When $kc_A/\Omega_+ \to 0$, (2.2) reproduces the single fluid hydromagnetic result of three uncoupled nondispersive waves; finite ion inertia couples and makes dispersive the three hydromagnetic waves.

Before considering finite ion inertia specifically, we compare the drift velocity with single fluid hydromagnetic wave speeds. For example, when $c_S{}^2/c_A{}^2$ is small, the fast wave speed is given approximately by $\omega^2 = k^2 c_A{}^2 + k_\perp{}^2 c_S{}^2$, where $k_\perp = k \sin\theta$. Since $\omega/k_\perp \gg v_p{}^{\pm}$ (when $R_+/L_p{}^{\pm} \ll 1$) for all angles of propagation, the fast wave weakly couples to drift motions. In general, hydromagnetic velocities are comparable with the thermal speeds, and so drift effects may be neglected. Propagation almost perpendicular to the magnetic field $(k_\perp \gg k_\parallel)$ is an exception. For example, $\omega = k_\parallel c_A$ for the intermediate wave for all angles of propagation; by choosing $k_\parallel/k_\perp \simeq R_+/L_p{}^{\pm} \ll 1$, we can reduce $\omega/k_\perp$ enough to be comparable with $v_p{}^{\pm}$. A similar argument applies to the slow wave; for example, when $c_S{}^2/c_A{}^2 \ll 1$, $\omega^2 = k_\parallel{}^2 c_S{}^2$; again ω is independent of $k_\perp$, so that increasing $k_\perp$ decreases $\omega/k_\perp$. Thus, the intermediate and slow waves have drift modifications when their perpendicular wavelength is much less than their parallel wavelength.

The above argument suggests that we need consider the effects of finite ion inertia only upon the nearly perpendicular intermediate and slow waves. When $k_\perp \gg k_\parallel$, $c_F{}^2 \gg \omega^2/k^2$ for these waves, and the bi-cubic (2.3) reduces to a biquadratic, removing the fast wave from consideration.

$$[c_I{}^2 - (\omega^2/k^2)]\ [c_{SL}^2 - (\omega^2/k^2)] = \frac{\omega^2}{k^2}\ [c_S{}^2 - (\omega^2/k^2)]\ r \tag{2.8}$$

where $r = \frac{k^2 c_A{}^2}{\Omega_+{}^2} \frac{c_I{}^2}{c_F{}^2}$ is a finite ion inertia parameter; $r \neq 0$ couples the intermediate and slow branches. The sign of the dispersive coupling depends upon the ratio of ω/k and c_S. Solving (2.8),

$$\frac{\omega^2}{k^2} = \frac{1}{1+r}\left\{\frac{c_I{}^2 + c_{SL}^2 + rc_S{}^2}{2} \pm \frac{c_I{}^2 - c_{SL}^2 + rc_S{}^2}{2} \times \right.$$

$$\left. \times \left[1 + \frac{4c_{SL}^2(c_S{}^2 - c_I{}^2)r}{[c_I{}^2(1+r) - c_{SL}^2]^2}\right]^{1/2}\right\} \tag{2.9}$$

When $0 < r << 1$, the intermediate wave is given by

$$\frac{\omega^2}{k^2} = c_I{}^2\left(1 + r\frac{c_S{}^2 - c_I{}^2}{c_I{}^2 - c_{SL}^2}\right) \tag{2.10}$$

Since $c_I{}^2 - c_{SL}^2 > 0$ always, intermediate wave speed increases as r increases if $c_S{}^2 > c_I{}^2$, and decreases if $c_S{}^2 < c_I{}^2$. $c_I{}^2 \equiv c_A{}^2 \cos^2\theta$ implies that when $c_S{}^2/c_A{}^2 < 1$, waves with $0 \leq \cos^2\theta < c_S{}^2/c_A{}^2$ speed up, and those with $c_S{}^2/c_A{}^2 \leq \cos^2\theta$ slow down with increasing r. Similarly, when r is small, the slow wave is

$$\frac{\omega^2}{k^2} = c_{SL}^2\left(1 - r\frac{c_S{}^2 - c_{SL}^2}{c_I{}^2 - c_{SL}^2}\right) \quad . \tag{2.11}$$

Since $c_S{}^2 \geq c_{SL}^2$, the slow wave decreases its phase velocity with increasing r. As $r \to \infty$, the intermediate wave approaches an isotropic sound wave

$$\omega^2/k^2 = c_S{}^2 \tag{2.12}$$

and the slow wave approaches a wave resonance $(\omega \to \Omega_+ \cos\theta)$

$$\frac{\omega^2}{k^2} = \frac{c_F{}^2\, c_{SL}^2}{(k^2 c_A{}^2/\Omega_+{}^2)\; c_S{}^2} = \frac{\Omega_+{}^2 \cos^2\theta}{k^2} \tag{2.13}$$

since $c_F{}^2\, c_{SL}^2 = c_A{}^2\, c_S{}^2 \cos^2\theta$.

2.3) Polarizations

Here, we estimate the parallel wave electric field $\delta E_{\parallel}$, and the compressional component of the wave magnetic field, $\delta B_{\parallel}$. The ratio of $\delta E_{\parallel}$ to the electric field component in the direction of the perpendicular wave vector, $\delta E_{\perp}$, is (Stringer, 1963; Formisano and Kennel, 1969)

$$\frac{\delta E_{\parallel}}{\delta E_{\perp}} = \frac{\tau\,[1 - (k^2 c_I{}^2/\omega^2)]\,\cos\theta \sin\theta}{[(\omega^2/k^2 c_S{}^2) - 1] + \tau \sin^2\theta\,[1 - (k^2 c_I{}^2/\omega^2)]} \tag{2.14}$$

$$\tau = \frac{\gamma_- T^-}{\gamma_+ T^+ + \gamma_- T^-}$$

where the appropriate ω^2/k^2 from (2.3) must be substituted in (2.14).

In the hydromagnetic limit $(kc_A/\Omega_+ = 0)$, $\omega = kc_I$ precisely, whereupon (2.14) implies $\delta E_{\parallel} = 0$; this means hydromagnetic waves have no Landau resonance interactions. Thus, while their propagation may be affected by drift terms, hydromagnetic Alfven waves can have no drift instabilities (Kennel and Greene, 1966). Substituting (2.10) into (2.14), $\delta E_{\parallel}/\delta E_{\perp}$ is, to lowest order in kc_A/Ω_+ ,

$$\frac{\delta E_{\parallel}}{\delta E_{\perp}} \simeq \frac{k^2 c_A^{\ 2}}{\Omega_+^{\ 2}} \; \frac{c_I^{\ 2} \, c_S^{\ 2}}{c_F^{\ 2}(c_I^{\ 2} - c_{SL}^{2})} \; \tau \cos\theta \sin\theta \tag{2.15}$$

suggesting that strong resonant Alfven wave-particle couplings occur when $kc_A/\Omega_+ \simeq 1$. By contrast, the slow wave has $\delta E_{\parallel} \neq 0$, and consequently Landau resonance interactions, even when $kc_A/\Omega_+ << 1$. For example, when $c_S^{\ 2}/c_A^{\ 2} << 1$, $\delta E_{\parallel}/\delta E_{\perp} \simeq \tan\theta = k_{\parallel}/k_{\perp}$, implying that the slow ion acoustic wave is electrostatic, and has a zero wave magnetic field.

In this section, we removed the magnetosonic wave from consideration by assuming $c_F^{\ 2} >> \omega^2/k^2$; in the kinetic theory calculation, we will do so by constraining the wave compressional magnetic field amplitude, $\delta B_{\parallel}$, to be zero. (In hydromagnetics, the fast wave has a nonzero $\delta B_{\parallel}$, while the intermediate wave always has $\delta B_{\parallel} = 0$, and when $c_S^{\ 2}/c_A^{\ 2} << 1$, the slow wave has a small $\delta B_{\parallel}$. Thus, assuming $\delta B_{\parallel} = 0$ picks out only slow and intermediate waves.) If $k_{\perp}$ is in the y-direction, the hydromagnetic intermediate wave has $\delta B_x \neq 0$. From two-fluid theory,

$$\frac{\delta B_{\parallel}}{\delta B_x} = \left(1 - \frac{k^2 c_I^{\ 2}}{\omega^2} \right) \frac{\omega^2}{k^2 c_A^{\ 2}} \; \frac{\Omega_+ \tan\theta}{\omega} \quad ; \tag{2.16}$$

substituting (2.10) into (2.16), assuming $\cos\theta << 1$.

$$\frac{\delta B_{\parallel}}{\delta B_x} = \frac{kc_A}{\Omega_+} \; \frac{c_S^{\ 2} - c_I^{\ 2}}{c_S^{\ 2} + c_A^{\ 2}} \quad . \tag{2.17}$$

Thus, both (2.16) and (2.17) indicate the hydromagnetic Alfven wave has $\delta B_{\parallel} = 0$. When $c_S^{\ 2}/c_A^{\ 2} << 1$, $\delta B_{\parallel}$ is small even when $kc_A/\Omega_+ \simeq 1$. The slow wave is electrostatic when $c_S^{\ 2}/c_A^{\ 2} << 1$, implying a small $\delta B_{\parallel}$.

We may argue alternatively as follows: For perpendicular propagation, the slow wave reduces to a discontinuity across which pressure is conserved. If $c_S^{\ 2}/c_A^{\ 2}$ is small, the fractional change in particle pressure across the slow discontinuity is larger than that in the field strength.

2.4) Summary

1.) Finite ion inertia dispersion causes the intermediate wave speed to approach c_S at short wavelengths. If $c_S > c_I$, the phase speed increases to c_S with increasing kc_A/Ω_+. When $c_I > c_S$, the phase speed decreases to c_S with increasing kc_A/Ω_+. The first case is appropriate to the magnetosphere, where particle pressures are large. Finite ion inertia decreases the slow speed; the slow wave frequency is always less than $\Omega_+ \cos\theta$. These features are illustrated in figure 1.

2.) When $k_\parallel/k_\perp \simeq R_+/L_p^{\pm} \ll 1$, intermediate and slow waves can interact with drift motions. Magnetosonic waves have no significant drift interaction at any propagation angle.

3.) The slow wave has a nonzero $\delta E_\parallel$, which permits Landau resonance interactions.

4.) Drift Alfven instabilities could explain magnetically polarized micropulsations. However, $\delta E_\parallel = 0$ in the hydromagnetic limit, implying hydromagnetic Alfven waves have no Landau coupling to particles.

5.) Finite ion inertia couples the slow and intermediate branches, causing an exchange of polarizations. With increasing kc_A/Ω_+, the intermediate Alfven wave acquires a $\delta E_\parallel$ (from the almost electrostatic slow wave), permitting Landau interactions at short wavelengths, $kc_A/\Omega_+ \simeq 1$.

6.) $\delta B_{\parallel}$ is large for the fast wave, zero for the hydromagnetic intermediate wave, and small for the slow ion acoustic wave when $c_S^2/c_A^2 \ll 1$. These relations hold for finite kc_A/Ω_+ so long as c_S^2/c_A^2 is not too large.

3. Kinetic Theory of Drift Waves in a Uniform Magnetic Field

3.1) Introduction

Two-fluid theory, even extended to spatially inhomogeneous plasmas, describes neither resonant wave-particle interactions, nor perpendicular wavelengths near the ion thermal cyclotron radius. Therefore, we turn to kinetic theory, making as many simplifying assumptions as possible before performing the calculation; these are described in section 3.2. In section 3.3, we derive a dispersion relation for coupled drift ion acoustic (slow) and drift Alfven (intermediate) waves. Section 3.4 closes with a comparison with two-fluid theory and with previous work on drift instabilities.

3.2) Approximations

a.) Straightline magnetic geometry.

We take the equilibrium magnetic field in the z-direction of an (x,y,z) Cartesian coordinate system. The equilibrium is uniform in y with gradients only along x . (For radial magnetospheric gradients, x $\sim$ radius, y $\sim$ longitude, z $\sim$ direction along magnetic field.) By neglecting field curvature, we cannot find the parallel mode structure, important for relating ground and satellite micropulsation experiments. [Cummings et al. (1969) have in fact calculated the mode structure of hydromagnetic standing Alfven waves in the period range of interest here.] However, the instability is probably qualitatively described by straightline geometry. In a paper on electrostatic drift waves in curved magnetic geometry, Rutherford and Frieman (1968) indicate that curvature introduces no new electrostatic modes or instabilities but only modifies details of those previously found in straightline approximation. No curved field calculations to date (e.g., Rosenbluth, 1968; Rutherford and Frieman, 1968; Liu, 1969) treats either the electromagnetic polarizations or perpendicular wavelengths near the ion cyclotron radius, important here. Nonetheless, from general geometry experience, we can extract two points. First, Landau interactions in straightline geometry correspond to bounce resonance interactions in general geometry. Since the most unstable drift waves have long wavelengths parallel to the magnetic field, whose upper limit is the length of the line of force, the $k_\parallel v_\parallel$ in the Landau resonance condition, $\omega - k_\parallel v_\parallel = 0$, corresponds approximately to the bounce frequency of a particle mirroring near the earth. Second, general geometry calculations involve quantities averaged over the length of the tube of force, i.e., $\langle Q \rangle = \int \frac{d\ell}{|B|} Q$, where $d\ell$ is an element of length along the line of force. This averaging process emphasizes those points where $|B|$ is small, suggesting that equatorial plane parameters make the appropriate correspondence between slab geometry calculations and the magnetosphere.

b.) Neglect of ionospheric attenuation and coupling.

We neglect wave energy losses due to resistive ionospheric attenuation or to coupling to the ionosopheric wave guide. To overcome any such losses and ensure instability, the equatorial plane growth rate must be finite and positive. However, if ionospheric losses are not strongly frequency dependent, the equatorial growth rate determines which modes are most unstable.

c.) Assumption of small magnetic inhomogeneity.

We assume $v_D^{\pm} << v_p^{\pm}$. This requires that $\frac{d\ \ell n\ p}{dx} >> \frac{d\ \ell n\ B}{dx}$. The hydromagnetic pressure equilibrium condition, $\nabla[p + (B^2/8\pi)] = 0$, implies for slab geometry, that $\left| \frac{d\ \ell n\ p}{dx} \right| \simeq \frac{2}{\beta} \frac{d\ \ell n\ B}{dx}$, where $\beta = 8\pi p/B$. Thus, if $\beta << 1$, $|\underset{\sim}{v}_D^{\pm}| << |\underset{\sim}{v}_p^{\pm}|$. For the inner edge of the electron plasma sheet, where $N \sim 1/cm^3$, $T^- \simeq 3$ keV , $B \simeq 60\gamma$, $\beta \simeq 0.3$, suggesting that $|\underset{\sim}{v}_p| \simeq 0(5)\ |\underset{\sim}{v}_D|$. In other words, when the electron $\beta < 1$, the logarithmic gradient of the magnetic field is roughly that of the dipole field. At $L \simeq 6$, the dipole scale length is $\simeq 2\ R_E$, whereas the electron scalelength is $\lesssim \frac{1}{2}\ R_E$ (Vasyliunas, 1968a). Our analysis is restricted to such sharp particle distribution gradients.

d.) Annihilation of fast magnetosonic wave.

The magnetosonic mode is always faster than typical drift speeds, and does not have large drift modifications; its presence only clutters drift calculations with irrelevant terms. We remove it <u>in advance,</u> by constraining the modes we do treat to have at most rotational magnetic field components, i.e., by requiring $\delta B_{\parallel} = 0$. Recall that only the fast wave has a significant nonzero $\delta B_{\parallel}$. An alternative argument is that the fast wave adjusts the total pressure time scales shorter than drift time scales, leaving only small $\delta B_{\parallel}$ adjustments to the other two waves.

e.) Localization of spatial eigenfunctions.

Because the plasma equilibrium is inhomogeneous, an integrodifferential equation describes, in general, the x-dependence of the waves' spatial eigenfunctions. For short x-wavelengths relative to equilibrium scale lengths, the WKB approximation, wherein the wave fields vary as $\exp i \left[\int^x k_x(x')\, dx' + k_y y + k_z z - \omega t\right]$, may be used. Since the instability energy source is a localized spatial gradient, the fastest growing modes should have eigenfunctions localized near the maximum plasma gradient. For these waves, the WKB dispersion relation has the form

$$\int_{x_1}^{x_2} dx'\, k_x(x';\omega,k_y,k_z) = n\pi$$

$$k_x(x_1) = k_x(x_2) = 0 \tag{3.1}$$

where the wave amplitude must tend to zero as $x \to \pm\infty$. Rukhadze and Silin (1964), Mikhailovsky (1967), Krall (1968), and others have argued that a good estimate of the eigenfrequencies and growth rate can be obtained by examining the turning points, where $k_x = 0$. Therefore, we set $k_x = 0$ in advance, creating an algebraic dispersion relation, rather than an integrodifferential equation with boundary conditions.

Combining the $\delta B_{\parallel} = 0$ and $k_x = 0$ conditions with Faraday's law implies that δE_x, which carries the fast wave, is zero. The only remaining wave components are δE_y, $\delta E_z \equiv \delta E$, δB_x, $k_y \equiv k_\perp$, and $k_z \equiv k_\parallel$.

3.3) Calculation of Dispersion Relation

The equilibrium distribution functions $F_o^{\pm}$ depend only upon the particle constants of motion. Time invariance and translational invariance along $\underset{\sim}{B}$ imply the particle energy and parallel momentum, respectively, are conserved; in nonrelativistic plasmas, $v_\perp$ and $v_\parallel$ are equivalent constants of motion. From y-invariance, $p_y = M_\pm v_y + eA_y/c$

is conserved. For a constant magnetic field, the vector potential $A_y = |B|x$, so that $X = x + (v_y/\Omega_\pm)$ is an equivalent constant of motion. We choose $F_o^{\pm}$ to be locally bi-Maxwellian:

$$F_o^{\pm}(X,v\ ,v\ ) = N \left[\frac{M_\pm}{2\pi T_\perp^{\pm}}\right] \left[\frac{M_\pm}{2\pi T_\parallel^{\pm}}\right]^{1/2} \exp - \left[\frac{M_\pm v_\perp^2}{2T_\perp^{\pm}} \quad \frac{M_\pm v_\parallel^2}{2T_\parallel^{\pm}}\right] \tag{3.2}$$

$N(X)$ is the electron and ion number density, and $T_\perp^{\pm}(X)$ and $T_\parallel^{\pm}(X)$, the electron or ion perpendicular and parallel temperature, respectively. The equilibrium particle orbits in the frame for which equilibrium electric fields are zero, are:

$$v_x = v_\perp \cos(\psi-\Omega_\pm t) \ ; \quad v_y = v_\perp \sin(\psi-\Omega_\pm t) \ , \quad v_z = v_\parallel \tag{3.3}$$

$$\begin{aligned} x(t) &= x_o - \frac{v_\perp}{\Omega_\pm}[\sin(\psi-\Omega_\pm t) - \sin\psi] \\ y(t) &= y_o + \frac{v_\perp}{\Omega_\pm}[\cos(\psi-\Omega_\pm t) - \sin\psi] \\ z(t) &= z_o + v_\parallel t \end{aligned} \tag{3.4}$$

where ψ is the Larmor phase at $t = 0$, and (x_o,y_o,z_o) is the particle location at $t = 0$. Finally,

$$X = x(t) + \frac{v_\perp \sin(\psi-\Omega_\pm t)}{\Omega_\pm} \tag{3.5}$$

For small amplitude harmonic wave fields, varying as $e^{i(\underset{\sim}{k}\cdot\underset{\sim}{x}-\omega t)}$, the wave electric field satisfies

$$\underset{\sim}{k} \times (\underset{\sim}{k} \times \delta\underset{\sim}{E}) + \frac{\omega^2}{c^2}\underset{\approx}{\varepsilon} \cdot \delta\underset{\sim}{E} = 0 \tag{3.6}$$

where the dielectric tensor $\underset{\approx}{\varepsilon}$ is defined by (Stix, 1962)

$$\underset{\approx}{\varepsilon}\cdot\delta\underset{\sim}{E} = \delta\underset{\sim}{E} + \frac{4\pi i}{\omega}\,\delta\underset{\sim}{J} = \delta\underset{\sim}{E} + \frac{4\pi i}{\omega}\, e \int d^3\underset{\sim}{v}\ \underset{\sim}{v}(\delta f^+ - \delta f^-) \tag{3.7}$$

$\delta\underset{\sim}{J}$ is the perturbation current, and $\delta f^{\pm}$, the perturbed distribution function. We treat one species of singly charged ions. The dispersion relation involves finding $\delta f^{\pm}$, multiplying by $\underset{\sim}{v}$, integrating over velocity space, expressing $\delta\underset{\sim}{J}$ in terms of $\delta\underset{\sim}{E}$, and solving the determinant of (3.6).

$\delta f^{\pm}$ can be found by the method of characteristics (Rosenbluth, 1965; Mikhailovsky, 1967), wherein $\delta f^{\pm}$ at $t = 0$ is given by an integration following unperturbed particle trajectories:

$$\delta f^{\pm}[\underset{\sim}{x}(t{=}0),\underset{\sim}{v}(t{=}0),0] = \mp \int_{-\infty}^{0} dt'\,\frac{e}{M_{\pm}}\left[\delta\underset{\sim}{E} + \frac{\underset{\sim}{v}(t')\times\delta\underset{\sim}{B}}{c}\right]\cdot\frac{\partial F_o^{\,\pm}}{\partial\underset{\sim}{v}}$$

$$\exp\left(i[k_{\perp}y(t') + k_{\parallel}z(t') - \omega t']\right) \tag{3.8}$$

where t' is a time index following particle trajectories. $\mathrm{Im}\,\omega = \gamma$ is assumed positive to ensure convergence of the integral at $t' = -\infty$.

Assuming $\delta E_x = \delta B_z = \delta B_y = 0$, using Faraday's law to express δB_x in terms of δE_y and δE_z, and making the change of coordinates $F_o^{\,\pm}[\underset{\sim}{x}(t),\underset{\sim}{v}(t)] \to F_o^{\,\pm}(X,v_{\perp},v_{\parallel})$ so that $F_o^{\,\pm}$ is a constant in the t' integration:

$$\mp\,\frac{e}{M_{\pm}}\left[\delta\underset{\sim}{E} + \frac{\underset{\sim}{v}\times\delta\underset{\sim}{B}}{c}\right]\cdot\frac{\partial F_o^{\,\pm}}{\partial\underset{\sim}{v}} = M^{\pm}\sin(\psi-\Omega_{\pm}t) + N^{\pm} \tag{3.9}$$

where

$$M^{\pm} = \mp\,\frac{e}{M_{\pm}}\left\{E_y\,\frac{\partial F_o^{\,\pm}}{\partial v_{\perp}} - \frac{(k_{\parallel}E_y - k_{\perp}E_z)}{\omega}\left[v_{\parallel}\,\frac{\partial F_o^{\,\pm}}{\partial v_{\perp}} - v_{\perp}\,\frac{\partial F_o^{\,\pm}}{\partial v_{\parallel}}\right]\right\}$$

$$N^{\pm} = \mp\,\frac{e}{M_{\pm}}\left\{E_{\parallel}\,\frac{\partial F_o^{\,\pm}}{\partial v_{\parallel}} + \frac{E_y}{\Omega_{\pm}}\,\frac{\partial F_o^{\,\pm}}{\partial X} - \frac{(k_{\parallel}E_y - k_{\perp}E_z)}{\omega}\,\frac{v_{\parallel}}{\Omega_{\pm}}\,\frac{\partial F_o^{\,\pm}}{\partial X}\right\} \tag{3.10}$$

For the locally bi-Maxwellian distributions, (3.2),

$$M^{\pm} = \pm \frac{e}{M_{\pm}} \frac{v_{\perp}}{(c_{\perp\pm})^2} \left\{ E_y \left[1 + \frac{k_{\parallel} v_{\parallel}}{\omega} A^{\pm} \right] - E_z \frac{k_{\perp} v_{\parallel}}{\omega} A^{\pm} \right\} F_o^{\pm}$$

$$N^{\pm} = \pm \frac{e}{M_{\pm}} \left\{ \frac{v_{\parallel} E_{\parallel}}{(c_{\parallel\pm})^2} \left[1 - \frac{k_{\perp} (c_{\parallel\pm})^2}{\omega \Omega_{\pm}} \frac{\partial}{\partial X} \right] - \frac{(\omega - k_{\parallel} v_{\parallel})}{\omega \Omega_{\pm}} E_y \frac{\partial}{\partial X} \right\} F_o^{\pm} \tag{3.11}$$

where the thermal speeds $c_{\perp\pm}$, $c_{\parallel\pm}$ are

$$c_{\perp\pm} = (T_{\perp}^{\pm}/M_{\pm})^{1/2} \quad , \quad c_{\parallel\pm} = (T_{\parallel}^{\pm}/M_{\pm})^{1/2} \tag{3.11a}$$

and the thermal anisotropy $A^{\pm}$ is $(T_{\parallel}^{\pm} - T_{\perp}^{\pm})/T_{\parallel}^{\pm}$. Note that

$$\frac{\partial F_o^{\pm}}{\partial X} = \frac{\partial \ln N}{\partial X} \left\{ 1 - \eta_{\perp}^{\pm} \left[1 - \frac{1}{2} (v_{\perp}/c_{\perp\pm})^2 \right] - \frac{\eta_{\parallel}^{\pm}}{2} \left[1 - \frac{v_{\parallel}^2}{(c_{\parallel\pm})^2} \right] \right\}$$

$$\eta_{\perp}^{\pm} = \frac{\partial \ln T_{\perp}^{\pm}}{\partial \ln N} \quad ; \quad \eta_{\parallel}^{\pm} = \frac{\partial \ln T_{\parallel}^{\pm}}{\partial \ln N} \tag{3.12}$$

Using (3.4), we may write

$$e^{i\underset{\sim}{k}\cdot\underset{\sim}{x}(t')-\omega t'} = e^{i\underset{\sim}{k}\cdot\underset{\sim}{x}_o} \sum_{n,m} J_n J_m \, e^{i(n-m)[\psi+(\pi/2)]} \, e^{-i(\lambda+n\Omega_{\pm})t'} \tag{3.13}$$

$$\lambda = \omega - k_{\parallel} v_{\parallel}$$

$$J_n \equiv J_n(k_{\perp} v_{\perp}/\Omega_{\pm}) \quad , \qquad m,n \text{ any integers}$$

where we used the Bessel function identity $e^{ia \sin\phi} = \sum_n J_n(a)\, e^{in\phi}$ twice. Combining (3.13) with (3.9), we perform the orbit integration noting that $F_o^{\pm}(X,v_{\perp},v_{\parallel})$ is independent of t' :

$$\delta f_k^{\pm}(x_o,y_o,z_o,v_\perp,v_\parallel,\psi) =$$

$$= i \sum_{n,m} \frac{J_m \, e^{i(n-m)[\psi+(\pi/2)]}}{\lambda + n\Omega_\pm} \left[- \frac{n\Omega_\pm}{k_\perp v_\perp} J_n M^{\pm} + N^{\pm} J_n \right] e^{ik\, y_o + ik\, z_o} \tag{3.14}$$

The perturbation currents are

$$\delta J_y = \sum_{+,-} (\pm e) \int d^3v \;\; v_\perp \sin\psi \; \delta f^{\pm}$$

$$= i \sum_{+,-} (\pm e) \sum_n \int \frac{d^3v \; v_\perp}{\lambda + n\Omega_\pm} \left[\frac{n^2 \, \Omega_\pm^{\,2}}{k_\perp^{\,2} \; v_\perp^{\,2}} J_n^{\,2} M^{\pm} - \frac{n\Omega_\pm}{k_\perp v_\perp} J_n^{\,2} N^{\pm} \right] \tag{3.15}$$

$$\delta J_z = \sum_{+,-} (\pm e) \int d^3v \; v_\parallel \; \delta f^{\pm}$$

$$= i \sum_{+,-} (\pm e) \sum_n \int \frac{d^3v \; v_\parallel}{\lambda + n\Omega_\pm} \left[- \frac{n\Omega_\pm}{k_\perp v_\perp} J_n^{\,2} M^{\pm} + J_n^{\,2} \hat{N}^{\pm} \right] \tag{3.16}$$

Equations (3.15) and (3.16) contain $v_\perp$-integrations over $F_o^{\pm}$, which contains $v_\perp$ directly and also indirectly through X . In evaluating (3.15) and (3.16) we assume the equilibrium scale length is much longer than the ion cyclotron radius, so that $F_o^{\pm}(X) \simeq F_o^{\pm}(x) + O(v_\perp/\Omega_+ L_p)$, and $\partial/\partial X \simeq \partial/\partial x$, thereby neglecting the indirect $v_\perp$ dependence.

When ω , γ , and the "bounce" frequencies $k_\parallel v_\parallel$ of typical particles are well below the ion cyclotron frequency, $\lambda/\Omega_\pm \ll 1$, and we may expand the summation of cyclotron resonance denominators:

$$\sum_n \frac{1}{\lambda + n\Omega_\pm} = \frac{\delta_{no}}{\lambda} + \sum_n \frac{(1-\delta_{no})}{n\Omega_\pm} \left(1 - \frac{\lambda}{n\Omega_\pm} + \dots \right) \tag{3.17}$$

where $\delta_{no} = 1$ if $n = 0$ and zero otherwise. Equation (3.17) implies that we neglect all cyclotron resonance interactions. For perpendicular wavelengths near the ion cyclotron radius, none of the ion Bessel functions are small; thus we must sum contributions from all n. However, this is faciliated using

$$\sum_n n\, J_n^{\,2} = \sum_n \frac{(1-\delta_{no})}{n} J_n^{\,2} = 0 \;;$$

$$\sum_n J_n^{\,2} = 1 \;;$$

$$\sum_n (1-\delta_{no})\, J_n^{\,2} = 1 - J_o^{\,2}$$

Keeping the first nonvanishing terms in $\lambda/\Omega_\pm$, (3.15) and (3.16) reduce to

$$\delta J_y = i \sum_{+,-} (\pm e) \int d^3v\, v_\perp \left[\frac{(1-J_o^{\,2})}{k_\perp v_\perp^{\,2}} \left[-\lambda M^\pm + k_\perp v_\perp N^\pm\right] \right] \tag{3.18}$$

$$\delta J_z = i \sum_{+,-} (\pm e) \int \frac{d^3v\, v_\parallel}{k_\perp v_\perp} \left[(J_o^{\,2} - 1)\, M^\pm + \frac{k_\perp v_\perp J_o^{\,2} N^\pm}{\lambda} \right] \tag{3.19}$$

The corrections to (3.18) and (3.19) are at least $0(\lambda/\Omega_\pm)$ smaller than the terms kept. Note that the y-current, which is responsible for Alfven waves, has no $1/\lambda$ Landau resonance terms, whereas the z-current, which leads to slow ion sound waves, does.

The relevant components of $\underset{\approx}{\varepsilon}$ are:

$$\varepsilon_{yy} = 1 + \sum_{+,-} \frac{\omega_{p\pm}^2}{\Omega_\pm^2} \left\{ G^\pm \left[1 + \frac{k_\parallel^{\,2}}{\omega^2} \left(\frac{T_\parallel^{\,\pm} - T_\perp^{\,\pm}}{M_\pm} \right) \right] - \frac{\omega^*_\pm}{\omega} \right\} \tag{3.20a}$$

$$\varepsilon_{yz} = \varepsilon_{zy} = - \sum_{+,-} \frac{\omega_{p\pm}^2}{\Omega_\pm^2}\, G^\pm\, \frac{k_\perp k_\parallel}{\omega^2} \left(\frac{T_\parallel^{\,\pm} - T_\perp^{\,\pm}}{M_\pm} \right) \tag{3.20b}$$

$$\varepsilon_{zz} = 1 + \sum_{+,-} \frac{\omega_{p\pm}^2}{\Omega_\pm^2} G^\pm \frac{k_\perp^2}{\omega^2} \left(\frac{T_\parallel^\pm - T_\perp^\pm}{M_\pm} \right) - D_S(\omega,k) \tag{3.20c}$$

$G^\pm$, which arises from $v_\perp$-integration of $(1-J_o^2)F_o^\pm$ is

$$G^\pm \equiv \frac{1 - e^{-z^\pm} I_o(z^\pm)}{z^\pm} \equiv \frac{1 - \Gamma_o^\pm}{z^\pm} \tag{3.21}$$

where $z^\pm \equiv k_\perp^2 T_\perp^\pm / M_\pm \Omega_\pm^2$, $\Gamma_n^\pm = e^{-z^\pm} I_n(z^\pm)$, and I_n is a modified Bessel function of the first kind. As $z^\pm \to 0$, $G^\pm \to 1$; for $z^\pm >> 1$, $G^\pm \sim 1/z^\pm$.

$\omega^*_\pm$ is a drift frequency:

$$\omega^*_\pm = \frac{k_\perp c_{\perp\pm}^2}{\omega\Omega_\pm} \int d^3v \frac{(1-J_o^2)}{z^\pm} \frac{\partial F_o^\pm}{\partial X} \simeq \frac{k_\perp c_{\perp\pm}^2}{\omega\Omega_\pm} \frac{d\, \ell n\, N}{dx} [G^\pm + \eta_\perp^\pm(\Gamma_o^\pm + \Gamma_1^\pm)] \tag{3.22}$$

where the arguments $z^\pm$ of $\Gamma_o^\pm$, $\Gamma_1^\pm$ have been suppressed. $D_S(\omega,k) = 0$ is the electrostatic drift wave dispersion relation;

$$D_S(\omega,k) = \sum_{+,-} \frac{\omega_{p\pm}^2}{c_{\parallel\pm}^2} \int \frac{d^3v\, v_\parallel^2\, J_o^2}{k_\parallel \omega N} \frac{[F_o^\pm - (k_\perp c_{\parallel\pm}^2/\omega\Omega_\pm)(\partial F_o^\pm/\partial X)]}{(\omega/k_\parallel) - v_\parallel} \tag{3.23}$$

Since, in reaching (3.20), we set all odd $v_\parallel$ moments of $F_o^\pm$ zero, we cannot treat instabilities from currents and heat flowing along lines of force.

Dropping terms small in M_-/M_+ (the largest of which is $O(M_-/M_+)^{1/2}$, comparable with terms of $O(\lambda/\Omega_+)$ already neglected), using $\Omega_+^2/\omega_{p+}^2 = c_A^2/c^2$ and dropping the unity terms in (3.20a) and (3.20c), which are of order $c_A^2/c^2 << 1$, we reduce (3.20) further:

$$\varepsilon_{yy} = \frac{c^2}{c_A^{\ 2}} \left[G^+ - \frac{\omega^*_+}{\omega} + \frac{k_\parallel^{\ 2}}{\omega^2} \frac{\tilde{\Delta T}}{M_+} \right] \tag{3.24a}$$

$$\varepsilon_{yz} = \varepsilon_{zy} = - \frac{c^2}{c_A^{\ 2}} \frac{k_\perp k_\parallel}{\omega^2} \frac{\tilde{\Delta T}}{M_+} \tag{3.24b}$$

$$\varepsilon_{zz} = \frac{c^2}{c_A^{\ 2}} \frac{k_\perp^{\ 2}}{\omega^2} \frac{\tilde{\Delta T}}{M_+} - D_S(\omega,k) \tag{3.24c}$$

$\tilde{\Delta T} \equiv \sum_{+,-} G^\pm (T_\parallel^{\ \pm} - T_\perp^{\ \pm})$ is an effective temperature anisotropy.

To correspond to frequencies between the ion and electron bounce frequencies, we assume $k_\parallel c_{\parallel +} \ll \omega \ll k_\parallel c_{\parallel -}$. For the intermediate speed to be smaller than the electron thermal speed $(c_A < c_{\parallel -})$, $8\pi N T_\parallel^{\ -}/B^2 = \beta_\parallel^{\ -} > 2(M_-/M_+)$. (Thus, overall, we require $1 \gg \beta_\parallel^{\ -} \gg 2(M_-/M_+)$.) For the slow speed to be larger than the ion thermal speed $(c_S > c_{\parallel +})$, $T_\parallel^{\ -}/T_\parallel^{\ +} > 1$. If, moreover, we assume $\gamma/\omega \ll 1$, then, for ions

$$\frac{1}{(\omega/k_\parallel) - v_\parallel} \simeq \frac{k_\parallel}{\omega} \left(1 + \frac{k_\parallel v_\parallel}{\omega} + \ldots\right) - i\pi \,\mathrm{sign}\, k_\parallel \, \delta[(\omega/k_\parallel) - v_\parallel] \tag{3.25a}$$

and, for electrons

$$\frac{1}{(\omega/k_\parallel) - v_\parallel} \simeq - \frac{1}{v_\parallel} \left(1 + \frac{\omega}{k_\parallel v_\parallel} + \ldots\right) - i\pi \,\mathrm{sign}\, k_\parallel \, \delta[(\omega/k_\parallel) - v_\parallel] \tag{3.25}$$

where the Dirac delta functions signify Landau resonance wave-particle interactions. Using (3.25), $D_S(\omega,k)$ becomes

$$D_S \simeq - \frac{\omega_{p+}^2}{\omega^2 k_\parallel^{\ 2} c_S^{\ 2}} \left[\Gamma_o^{\ -} \omega^2 - \tilde{\omega}_- \omega - k_\perp^{\ 2} c_S^{\ 2} \left(\Gamma_o^{\ +} - (\tilde{\omega}_+/\omega)\right) + i\delta\right] \quad . \tag{3.26}$$

Unlike the fluid definition (2.9), here $c_S^{\ 2} \equiv T_\parallel^{\ -}/M_+$. $\tilde{\omega}_+$ is an ion drift frequency:

$$\tilde{\omega}_+ = \frac{k_\perp c_{\parallel +}^2}{\omega\Omega_+} \int d^3v \, \frac{v_\parallel^2}{c_{\parallel +}^2} J_o^2 \frac{\partial F_o^+}{\partial X} \simeq \frac{k_\perp c_{\parallel +}^2}{\omega\Omega_+} \frac{d \,\ell n\, N}{dx} [\Gamma_o^+(1 + \eta_\parallel^+) - z^+\eta_\perp^+(\Gamma_o^+ + \Gamma_1^+)] \tag{3.27}$$

$\tilde{\omega}_-$ is the corresponding electron drift frequency

$$\tilde{\omega}_- = \frac{k_\perp c_{\parallel -}^2}{\omega\Omega_-} \frac{d \,\ell n\, N}{dx} [\Gamma_o^- - z^-\eta_\perp^- (\Gamma_o^- + \Gamma_1^-)] \tag{3.28}$$

In section 4, we will use the fact that when $z^- << 1$, $\tilde{\omega}_-$ is a pure number density drift. δ contains resonant ion and electron effects:

$$\delta = \sqrt{\pi/2} \, \frac{k_\parallel^2 c_S^2 \omega^2}{\omega_{p+}^2} \sum_{+,-} \left[\frac{\omega_{p\pm}}{k_\parallel c_{\parallel \pm}}\right]^2 \frac{\omega}{|k_\parallel| c_{\parallel\pm}} \exp[-\omega^2/2k_\parallel^2 c_{\pm}^2] \cdot$$
$$\cdot \left\{ \Gamma_o^\pm \left[1 - \frac{k_\perp c_{\parallel\pm}^2}{\omega\Omega_\pm} \frac{d \,\ell n\, N}{dx} \left(1 - \frac{\eta_\parallel^\pm}{2} [1 - (\omega^2/k_\parallel^2 c_{\parallel\pm}^2)] \right) \right] - \frac{k_\perp c_{\parallel\pm}^2}{\omega\Omega_\pm} \frac{d \,\ell n\, N}{dx} \eta_\perp^\pm z^\pm (\Gamma_o^\pm + \Gamma_1^\pm) \right\} \tag{3.29}$$

Using (3.20) - (3.29), we may find the dispersion relation:

$$[G^+\omega^2 - \omega\omega^*_+ - k_\parallel^2 \bar{c}_A^2] \, [\Gamma_o^-\omega^2 - \tilde{\omega}_-\omega - k_\parallel^2 c_S^2(\Gamma_o^+ - (\tilde{\omega}_+/\omega)) + i\delta]$$
$$= \frac{k_\perp^2 \bar{c}_A^2}{\Omega_+^2} k_\parallel^2 c_S^2 [G^+\omega^2 - \omega\omega^*_+] \tag{3.30}$$

where $\bar{c}_A$ is an effective Alfven speed reflecting modifications by thermal anisotropy ("firehose") and finite cyclotron radius effects,
$\bar{c}_A^2 = c_A^2 - \tilde{\Delta T}/M_+$.

3.4) Discussion

Let us compare (3.30) with homogeneous two-fluid theory results. Neglecting thermal anisotropies and spatial derivatives, (3.30) reduces to

$$[\omega^2 - (k_\parallel^{\,2} c_A^{\,2}/G^+)]\;[\Gamma_o^- \omega^2 - k_\parallel^{\,2}\, c_S^{\,2}\, \Gamma_o^{\,+} + i\delta] = \frac{k_\perp^{\,2}\, c_A^{\,2}}{\Omega}\, k_\parallel^{\,2}\, c_S^{\,2}\, \omega^2$$

(3.31)

Neglecting δ, and noting that when $z^\pm << 1$, G^+ and $\Gamma_o^{\,\pm}$ approach unity, (3.32) may be rewritten

$$[c_I^{\,2} - (\omega^2/k^2)]\;[c_{SL}^2 - (\omega^2/k^2)] = \frac{\omega^2}{k^2}\, c_S^{\,2}\, \frac{k_\parallel^{\,2}}{k^2}\, \frac{k_\perp^{\,2}\, c_A^{\,2}}{\Omega} \quad , \qquad (3.32)$$

using $c_{SL}^2 \simeq c_S^{\,2}\,(k_\parallel^{\,2}/k^2)$ when $c_S^{\,2}/c_A^{\,2} << 1$. When $c_A^{\,2} >> c_S^{\,2} >> \omega^2/k^2$, (3.32) and (2.8) reduce to approximately the same expression, with $k_\perp^{\,2} c_A^{\,2}/\Omega_+^{\,2}$ in (3.32) replacing $k^2 c_A^{\,2}/\Omega_+$ in (2.8). Since $k_\perp/k \simeq 1$, this difference is unimportant. Thus, kinetic theory reproduces homogeneous two fluid theory results when $c_S^{\,2}/c_A^{\,2}$ and $z^\pm$ are small, and resonant particles may be neglected.

Finite cyclotron radius (FCR) effects, not described in fluid theory, may be evaluated schematically by neglecting finite ion inertia in (3.31), whereupon when $z^- << 1$, the intermediate and slow waves are given by $\omega^2 = k_\parallel^{\,2} c_A^{\,2}/G^+$ and $\omega^2 = k_\parallel^{\,2} c_S^{\,2} \Gamma_o^{\,+}$ respectively. Both FCR and finite ion inertia increase the intermediate speed and decrease the slow speed as $k_\perp$ increases, since both G^+ and $\Gamma_o^{\,+}$ decrease as z^+ increases.

δ represents Landau wave-particle interactions, which in homogeneous Maxwellian plasmas can only damp waves. Spatial inhomogeneity, however, permits instability in certain cases. It also modifies the real part of the wave frequency, through ω^*_+ and $\tilde{\omega}_\pm$.

(3.30) reduces to the results of Mikhailovsky and Rudakov (1963), who kept finite inertia coupling but assumed $z^+ << 1$ and to those of Kennel and Greene (1966) who treated hydromagnetic drift instabilities ($z^+ \simeq kc_A/\Omega_+ \simeq 0$) for arbitrary $c_S{}^2/c_A{}^2$. When $z^- = \eta^{\pm} = \eta^{\pm} = \Delta\tilde{T} = 0$, (3.30) reproduces the results of Mikhailovsky (1967).

4. Drift Instabilities of the Auroral Electron Boundary

4.1) Alfven Thermal Gradient Instability

The auroral boundary electron temperature gradient is much larger than the number density gradient (Vasyliunas, 1968a). The ions have no sharp gradient near the electron boundary (Frank, 1968). Thus, we keep only the electron temperature gradient. Since when $z^- \ll 1$, $\tilde{\omega}_- \simeq 0$ for small number density gradient, (3.31) reduces to (3.32), the homogeneous plasma dispersion relation, except that δ has thermal gradient contributions. When $\gamma/\omega \ll 1$, (3.32) reduces to separate equations for γ and ω :

$$[\omega^2 - (k_\parallel{}^2 c_A{}^2/G^+)]\ [\omega^2 - k_\parallel{}^2\ c_S{}^2\ \Gamma_o{}^+] = \omega^2\ k_\parallel{}^2\ c_S{}^2\ (k_\perp{}^2 c_A{}^2/\Omega_+{}^2) \tag{4.1a}$$

$$\frac{\gamma}{\omega} = -\frac{\delta}{2}\ \frac{\omega^2 - (k_\parallel{}^2 c_A{}^2/G^+)}{[\omega^4 - (k_\parallel{}^4 c_A{}^2 c_S{}^2 \Gamma_o{}^+/G^+)]} \tag{4.1b}$$

where $\widetilde{\Delta T}$ is assumed zero. $\gamma > 0$ signifies instability. In order that $\gamma \neq 0$, $\omega^2 \neq k_\parallel^2 c_A{}^2/G^+$; this condition is always satisfied for the slow wave, and for the intermediate wave only when finite ion inertia is accounted for.

When $z^+ > 0$, both FCR and finite ion inertia ensure $\omega^2 > k_\parallel{}^2\ c_A{}^2$ and $\omega^2 < k_\parallel{}^2\ c_S{}^2$ for the intermediate and slow waves respectively. Since, moreover, $c_S{}^2/c_A{}^2 < 1$, we may decouple the two waves in (4.1a) by assuming $\omega^2 \gg k_\parallel{}^2\ c_S{}^2\ \Gamma_o{}^+$ for the Alfven wave, whereupon

$$\omega^2 = \frac{k_\parallel{}^2 c_A{}^2}{G^+} + \frac{k_\perp{}^2 c_A{}^2}{\Omega_+{}^2}\ k_\parallel{}^2 c_S{}^2 = k_\parallel{}^2\ c_A{}^2 \left[\frac{1}{G^+} + z^+\ \frac{T^-}{T^+}\right] \tag{4.2}$$

Similarly we may assume $\omega^2/k_\parallel^2 c_+^2 >> 1$, permitting neglect of ion Landau interactions. Then, substituting (4.2) into (4.1b)

$$\frac{\gamma}{\omega} = -\sqrt{\pi/8}\ \frac{\omega}{|k_\parallel| c_-}\ \exp[-\omega^2/2k_\parallel^2 c_-^2]\ \frac{k_\perp^2 c_A^2}{\Omega_+^2}\ \frac{k_\parallel^2 c_S^2}{\omega^2}\ \cdot$$

$$\cdot \left[1 + \frac{\Lambda}{\omega}\ [1 - (\omega^2/k_\parallel^2 c_-^2)] \right] \tag{4.3}$$

Λ is the electron temperature drift frequency

$$\Lambda = \frac{k_\perp c_-^2}{2\Omega_-}\ \frac{d\ \ell n\ T^-}{dx} \equiv \frac{T^-}{T^+}\ \sqrt{z^+}\ \frac{c_S}{2L_T} \tag{4.4}$$

where $L_T = (d\ \ell n\ T^-/dx)^{-1}$. When $\Lambda = 0$, the Alfven wave is damped. A sufficient condition for instability is

$$1 + \frac{\Lambda}{\omega}\ [1 - (\omega^2/k_\parallel^2 c_-^2)] < 0 \tag{4.5}$$

Since by assumption $\omega^2/k_\parallel^2 c_-^2 < 1$, $\Lambda/\omega < -1$ is a necessary condition for instability, implying that the perpendicular phase velocity $\omega/k_\perp$ and the thermal gradient drift velocity $c_-^2/2\Omega_-\ \frac{d\ \ell n\ T^-}{dx}$ are oppositely directed. $|\Lambda/\omega| > 1$ implies

$$\Delta_A \equiv \frac{T^-}{T^+}\ \frac{c_S}{c_A}\ \frac{1}{2k_\parallel L_T} > \left[\frac{1}{1 - \Gamma_o^+} + \frac{T^-}{T^+} \right]^{1/2} \tag{4.6}$$

Large Δ_A leads to instability. T^-/T^+ large, c_S/c_A large, and a large ratio of parallel wavelength to thermal gradient scalelength $(k_\parallel L_T << 1)$ all contribute to instability. When $z^+ << 1$, $\Gamma_o^+ \simeq 1 - z^+$ and $(1 - \Gamma_o^+)^{-1} \simeq 1/z^+$, so that instability does not occur for $z^+ \to 0$. z^+ must surpass a threshold value for instability; for instance, when

$\Delta_A = 2$, and $T^-/T^+ = 2$, $z^+ > 0.8$ for instability. Thus, except for very large Δ_A , instability sets in at wavelengths near the ion cyclotron radius. Since when $z^+ \gg 1$, both Λ and ω grow as $\sqrt{z^+}$ (for k constant), a necessary condition for large z^+ and thus any z^+ to be unstable is obtained by setting $\Gamma_o^+ \to 0$ in (4.6), $\Delta_A > \sqrt{1 + T^-/T^+}$.

For $k_\parallel$ constant, γ increases with increasing ω and z^+ until $\omega \approx k_\parallel c_-$, when γ changes sign. When $k_\parallel$ corresponds to the lowest parallel mode, the unstable wave frequencies are below the electron bounce frequency and above the larger of the Alfven bounce frequency, $k_\parallel c_A$, or the proton bounce frequency, $k_\parallel c_+$ (since ion Landau damping would kill the instability). Since γ maximizes just before it changes sign, the most unstable frequency is near but below the electron bounce frequency. In curved magnetic geometry, the growth rate peaks even more strongly near but below the bounce frequency since $\omega/|k_\parallel|c_-$ is replaced by a term of $O(\omega/k_\parallel c_-)^3$ (Rutherford and Frieman, 1968).

4.2) Ion Sound Thermal Gradient Instability

Assuming $\omega^2 \ll k_\parallel^2 c_A^2$, the slow ion sound wave frequency and growth rate are given by

$$\omega^2 = \frac{k_\parallel^2 c_S^2 \Gamma_o^+}{1 + (k_\perp^2 c_S^2/\Omega_+^2)\, G^+} = \frac{k_\parallel^2 c_S^2 \Gamma_o^+}{1 + (T^-/T^+)\,(1 - \Gamma_o^+)} \tag{4.7}$$

$$\frac{\gamma}{\omega} = -\sqrt{\frac{M_-}{M_+}\frac{\pi}{8}}\,(\omega/k_\parallel c_S)^3\,\frac{1}{\Gamma_o^+}\left[1 + \frac{\Lambda}{\omega} + (T^-/T^+)^{3/2}\,\Gamma_o^+\exp[-\omega^2/2k_\parallel^2 c_+^2]\right] \tag{4.8}$$

where we assumed $\omega/k_\parallel c_-$ very small, true except when T^-/T^+ is unrealistically large. A necessary condition for instability is $\Lambda/\omega < -1$, which requires

$$\Delta_S \equiv \frac{T^-}{T^+} \frac{1}{2k_\parallel L_T} > \left[\frac{\Gamma_o^{\,+}}{z^+[1 + (T^-/T^+)(1 - \Gamma_o^{\,+})]} \right]^{1/2} \tag{4.9}$$

This instability criterion, while less stringent than that for Alfven waves, still requires that z^+ be finite. Therefore, the unstable frequencies lie below $k_\parallel c_S$. As z^+ increases, $\omega/k_\parallel$ decreases to c_+, where the basic assumptions of this calculation break down. Thus, the lowest parallel mode will probably be unstable only above the ion bounce frequency.

5. Summary

Only the intermediate and slow wave branches have strong drift interactions. To do so, they must propagate nearly perpendicular to the magnetic field ($k_\parallel/k_\perp \simeq R_+/L_p << 1$). We restrict ourselves to c_S^2/c_A^2 small. Then, the slow wave is the ion sound wave, which always has a parallel electric field, and therefore, Landau interactions. On the Alfven branch, $\delta E_\parallel \neq 0$, permitting Landau resonance instabilities, only at short perpendicular wavelengths, where finite ion inertia coupling permits an exchange of polarization with the ion acoustic wave.

We derived the properties of drift Alfven and ion sound waves, coupled by finite ion inertia, in section 3. The various limitations of this theory are outlined in section 3.2; in particular, we neglect magnetic curvature, and the effects of magnetic gradient drifts. The second assumption restricts us to very sharp distribution function gradients, such as the auroral electron boundary. In the remainder of the magnetosphere, the density and magnetic drifts are comparable. In this case, the appropriate drift calculations must be generalizations of Rosenbluth, Krall and Rostoker (1962), who treated $k_\parallel = 0$ only, or of Kennel and Greene (1966), who treated only $z^+ << 1$. Mikhailovsky and Fridman (1968), have recently calculated the properties of high β drift waves with $V_D \neq 0$.

A great simplification occurs for the auroral electron boundary, since we may neglect all spatial gradients but that of the electron temperature. Here, the drift terms disappear from the real part of the dispersion relation, leaving it very similar to homogeneous two-fluid theory; however, the growth rate has a destabilizing contribution from the temperature gradient. Let us now compare the qualitative predictions of this theory with experiment.

5.1) Satisfaction of Instability Criterion

We compute Δ_A for parameters appropriate to the postmidnight auroral zone equatorial plane. For $T^- \approx 4$ keV , $T^+ \approx 1$ keV , $B = 70\ \gamma$, $N \approx 1/\mathrm{cm}^3$, $c_S \approx 8.6 \times 10^7$ cm/sec , $c_A \approx 4.8 \times 10^8$ cm/sec , and $c_S/c_A \approx .18$. The longest parallel wavelength available is the length of the line of force, $\approx 20\ R_E$ at $L = 6$. For this lowest parallel mode $\Delta_A \approx 1.1\ R_E/L_T$. From (4.6), $\Delta_A > \sqrt{1 + T^-/T^+} \approx 2.2$ implies instability. Thus, if $L_T < 0.5\ R_E$, Alfven wave instability is possible. Observed values of L_T fall within this range (Vasyliunas, 1968a). On the other hand, higher parallel modes are not likely to be unstable for this range of parameters.

5.2) Unstable Frequencies and Wavelengths

When only the lowest parallel mode is excited, the unstable frequency range should be narrow, lying above the Alfven bounce frequency $(k_\parallel c_A)$ and the thermal electron bounce frequency $(k_\parallel c_-)$. For the parameters chosen above, these two outer limits correspond to periods of 4 and 25 seconds. Since the growth rate maximizes near but below $k_\parallel c_-$, waves with ≈ 10 second periods should dominate the spectrum. McPherron et al. (1968) have characterized the observed micropulsations as "band-limited" in the 5-15 second period range.

Corresponding to the narrow unstable frequency range, a small range of perpendicular wavelengths, approximately $1 < \sqrt{z^+} < c_-/c_A$ (cf. Section 4.2), should be unstable: perpendicular wavelengths near the thermal proton cyclotron radius in the equatorial plane, some tens of kilometers.

5.3) Location, Localization, and Propagation

The association with the inner edge of the plasma sheet suggests that Alfven micropulsations will be located equatorward of the main auroral activity, in agreement with the location of auroral light pulsations (Cresswell and Davis, 1966). The fastest growing modes will be localized in radius to the region of maximum electron temperature gradient. If the equatorial thermal scalelength is $\frac{1}{2} R_E \simeq 3000$ km , the ionospheric scalelength is the order of 100 km, consistent with the localization of energetic electron precipitation pulsations (Barcus et al., 1965; Barcus et al., 1966; Parks et al., 1968a) and of 10 second auroral light modulations (Cresswell and Davis, 1966).

Since the instability criterion (4.6) involves T^-/T^+ , the steady convection electric field across the magnetosphere (Axford and Hines, 1961) could account for the observed diurnal occurrence pattern for 5-15 second micropulsations. Electrons are accelerated on the morning side and ions on the evening side (Brice, 1968). Thus, if $T^-/T^+ \simeq 1$ in the magnetospheric tail, $T^-/T^+ > 1$ on the morning side and $T^-/T^+ < 1$ on the evening side. Choosing $T^- \simeq 1$ keV and $T^+ \simeq 4$ keV with all other parameters the same as above, $\Delta_A \simeq .03\, R_E/L_T$, strongly suggesting that instability is not possible. 5-15 second auroral micropulsations are observed primarily in the 0200-1000 L.T. postmidnight sector (McPherron et al., 1968). Thus, while the auroral electron boundary is more pronounced on the evening side (Vasyliunas, 1968a) than on the morning side (Vasyliunas, 1968b), it appears that the electron to ion temperature ratio may play the controlling role in determining instability.

If we assume the eigenoscillation is a standing wave in x (radius) and z (along the lines of force), then energy propagates along y , or in longitude. From (4.5), the unstable waves propagate opposite to the electron thermal gradient drift, or towards morning, with phase velocities less than $\Lambda/k_\perp \simeq 10$ km/sec, in the equatorial plane. This velocity, mapped onto the ionosphere, is $\simeq 1$ km/sec. If the micropulsations modulate electron precipitation, then the phase surfaces of associated auroral light irregularities should progress eastward at near but below this velocity. Cresswell and Davis (1966) found pulsating auroras move eastward with 0.1 - 1 km/sec velocities. The fact that no north-south motions were observed is consistent with a radially confined mode.

5.4) Polarization

Our calculation keeps only δB_x , corresponding to a radial perturbation magnetic field in the equatorial plane, which maps into a north-south perturbation field in the ionosphere if there is no rotation of the polarization along the line of force. Accurate calculations of the x-dependence of the eigenfunction are needed to determine the actual δB_y , or longitudinal component. In any case, the rotational components of the perturbation field should be larger than the compressional components, though because c_S/c_A is not always small, $\delta B_\parallel$ is not necessarily strictly zero, as was assumed here. 5-15 second band limited micropulsations are observed magnetically on the ground (McPherron et al., 1968), consistent with a magnetic polarization in space.

5.5) Estimate of Saturation Amplitude

The development of the drift instability should smooth the electron temperature gradient driving it, by diffusing particles across lines of force. Assuming this process is incoherent, we can write an approximate heat flow equation

$$\frac{\partial T^-}{\partial t} = D \frac{\partial^2 T^-}{\partial x^2} \tag{5.1}$$

where the heat conduction coefficient should be given dimensionally by the magnitude of the particle velocities in the wave $(c\delta E/B_o)$ and the wave frequency $D \simeq (c\delta E/B_o)^2 \omega^{-1}$. In the strong diffusion picture of the auroral electron boundary (Petschek and Kennel, 1966; Kennel, 1969; Vasyliunas, to be published) the minimum lifetime for electron precipitation T_M is the scale time for boundary formation. Assuming that thermal transport also has this scale time permits a crude estimate of the amplitude.

Equating $T_M \simeq L_T^2/D \simeq 10^3$ sec (for L = 6 and keV electrons), and noting $\delta E \simeq (c_A/c)\,\delta B$,

$$T_M \simeq (L_T/c_A)^2\, \omega(\delta B/B_o)^{-2} \tag{5.2}$$

For $L_T = 0.5\ R_E$, $\omega = 2\pi/10$ radians/sec, $c_A \simeq 2 \times 10^8$ cm/sec, $\delta B/B_o \simeq .03$, or $\delta B \simeq 3\ \gamma$ when $B_o = 10^2\ \gamma$. This wave amplitude ought to be dominantly rotational. Ground based measurements indicate $\delta B \simeq 1\ \gamma$ (McPherron, private communication). Let us now ask whether Alfven micropulsations can create an electron precipitation pulsation. To achieve an effective compressional magnetic component the Alfven wave must carry particles into an increasing part of the dipole field. In this case, the effective compressional amplitude b, defined in Coroniti and Kennel (1969), is

$$b \simeq B_o \frac{3\lambda_\perp}{LR_E} \qquad (5.3)$$

where $\lambda_\perp$ is the perpendicular wavelength. Choosing $B_o \simeq 10^2\ \gamma$, $\lambda \simeq 30$ km (approximately a 1 keV ion cyclotron radius), $R_E = 6 \times 10^3$ km, and $L = 6$, we find $b \simeq 1.5\ \gamma$, consistent with their estimate for electron precipitation pulsations with peak-to-valley flux ratios of 2. Thus, if this picture is correct, whistler amplitudes ought occasionally to be modulated by Alfven micropulsations. Brody et al. (1969) have reported preliminary observations of whistler chords bursts, which repeat quasi-periodically with typically 6-11 second periods, in the postmidnight auroral equatorial plane. A schematic summary of these ideas is shown in figure 2.

5.6) Ion Sound Thermal Gradient Instability

According to (4.9), $k_{\parallel}L_T$ need not be as small for ion sound instability as for Alfven instability, suggesting that if Alfven waves are excited, so will lower frequency ion sound waves. However, if Alfven waves are somewhat above marginal stability, their growth rate is larger than the ion sound growth rate. Then, if waves with the largest growth rate dominate the developed spectrum, or if ionospheric damping is important, the ion sound component may not be apparent. Since higher parallel ion sound modes could also be unstable, estimates of the unstable frequency spectrum must wait until curved magnetic field calculations with ionospheric damping are carried out. However an interesting, if extremely difficult, experimental question is raised: are there nearly electrostatic micropulsations?

Before the question of whether drift instabilities can account for various different micropulsations can be answered, several theoretical and experimental developments are necessary. Some of these necessary developments have been indicated by the present calculation. On the theoretical side, curved magnetic geometry calculations, including full electromagnetic polarizations, finite β, resonant particles, and short nonhydromagnetic wavelengths, must be carried out. The magnetic gradient and curvature guiding center drifts must also be retained, since the particle scalelengths will be longer than in the auroral electron boundary elsewhere in the magnetosphere. Even in the present calculation, neglect of the gradient drift presents some uncertainty, since the unstable waves propagate eastward with a velocity comparable with the guiding center drift velocity of Van Allen electrons of a few tens of keV energy. The loss of wave energy to the ionosphere should be evaluated. On the experimental side, the relationship of spatial gradients in the particle distributions to micropulsation activity needs to be elucidated. The question of electrostatic micropulsations is unresolved experimentally. Here the association with precipitation pulsations could prove quite useful, since particle modulations in the absence of magnetic oscillations could be evidence for electrostatic micropulsations. Nevertheless, despite these technical obstacles, drift instabilities appear to be a serious candidate for various micropulsations. An instability analysis of the auroral electron boundary, the one case where the particle gradient is experimentally well-defined and which fortuitously is open to the limited analytic techniques used here, has led us to propose a wave generation mechanism which is at least not inconsistent with the observations of period, spatial location and localization, and propagation speed and direction, of a common auroral micropulsation.

Acknowledgments

This work was begun at the AVCO-Everett research laboratory, under NASA Nasw-1400, and continued (by FVC) at University of California, Berkeley, under NASA NSG-243 and NGL-05-003-012, and at UCLA (FVC and CFK) under NGR-05-007-190.

We are grateful to R. L. McPherron and J. M. Cornwall for very many useful discussions.

Figure Captions

Figure 1. Oblique Hydromagnetic Waves with Ion Inertia.

These plots schematically summarize the effects of ion inertia on wave propagation nearly across the magnetic field in a homogeneous plasma. Figure 1a describes the $c_S/c_I > 1$ case ordinarily appropriate to the magnetosphere, and 1b, the $c_S/c_I < 1$ case. In both cases, the fast wave has much larger phase and group velocities than the slow and intermediate wave. In both cases, finite ion inertia converts the intermediate wave into an isotropic sound wave $(\omega/k = c_S)$, and drives the slow wave to an oblique ion cyclotron resonance, $\omega = \Omega_+ \cos\theta$. The slow and intermediate waves have a small compressional magnetic field component, $\delta B_{\parallel}$. EM denotes mixed electric and magnetic, and ES, approximately electrostatic polarization.

Figure 2. Disturbed Auroral Electron Boundary.

When the electron boundary is sharp enough, a drift Alfven instability creates $\approx$ 10 second period micropulsations, primarily after midnight. When unstable whistler turbulence is already present, the micropulsations modulate the whistler instability, leading to finite amplitude precipitation pulsations observable in the auroral ionosphere.

MICROPULSATION MODULATION
OF MICROSCOPIC TURBULENCE

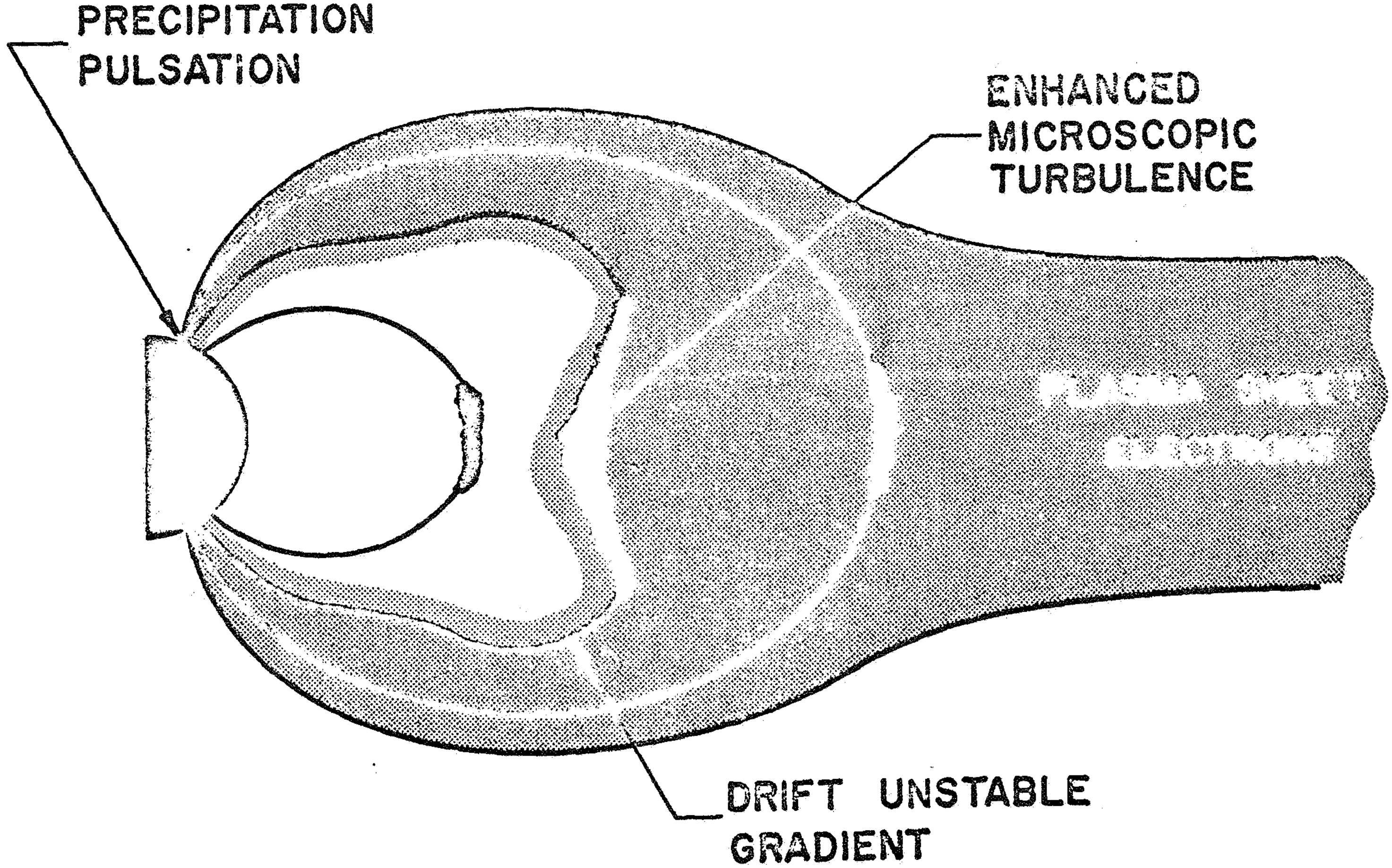

OBLIQUE HYDROMAGNETIC WAVES WITH
ION INERTIA

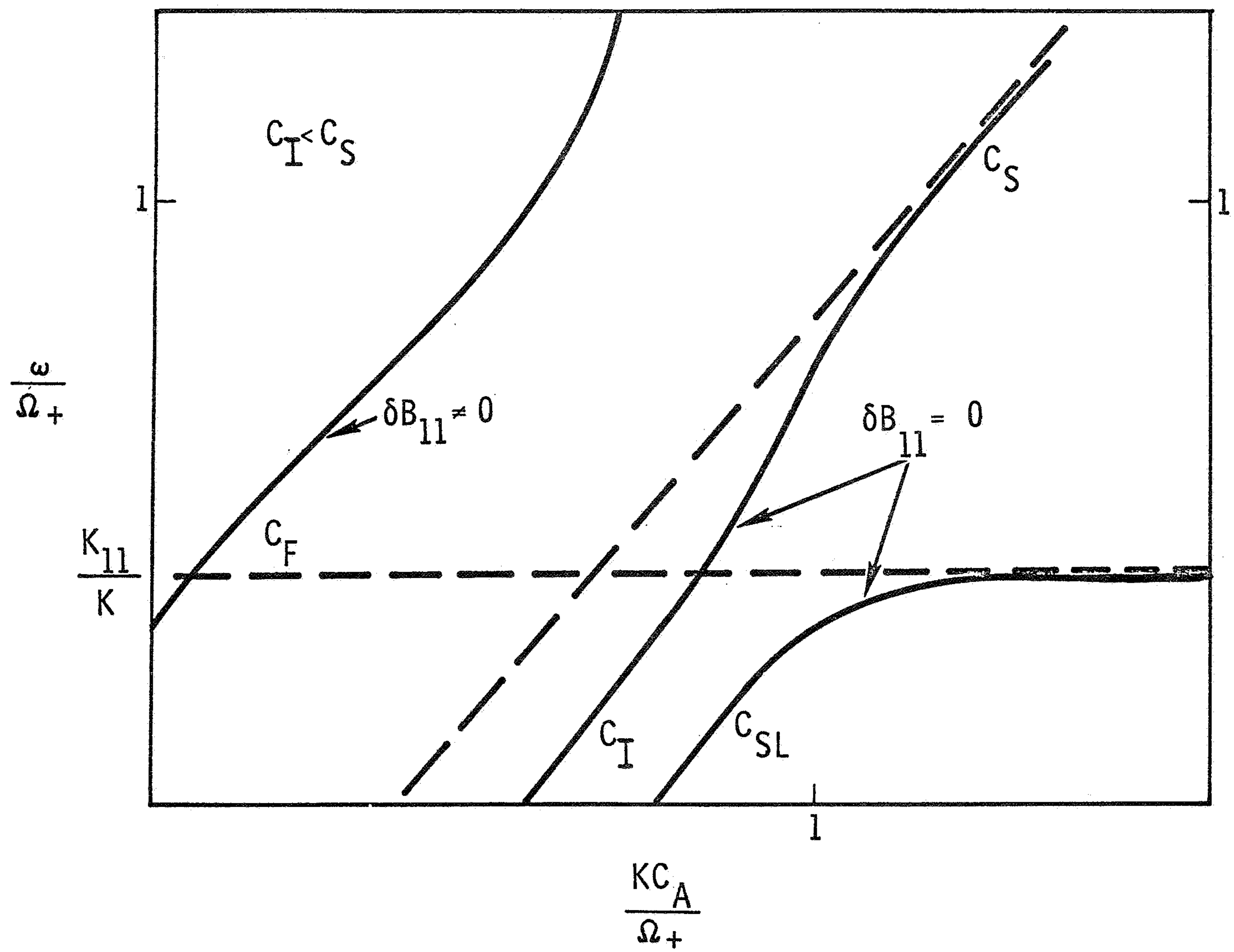

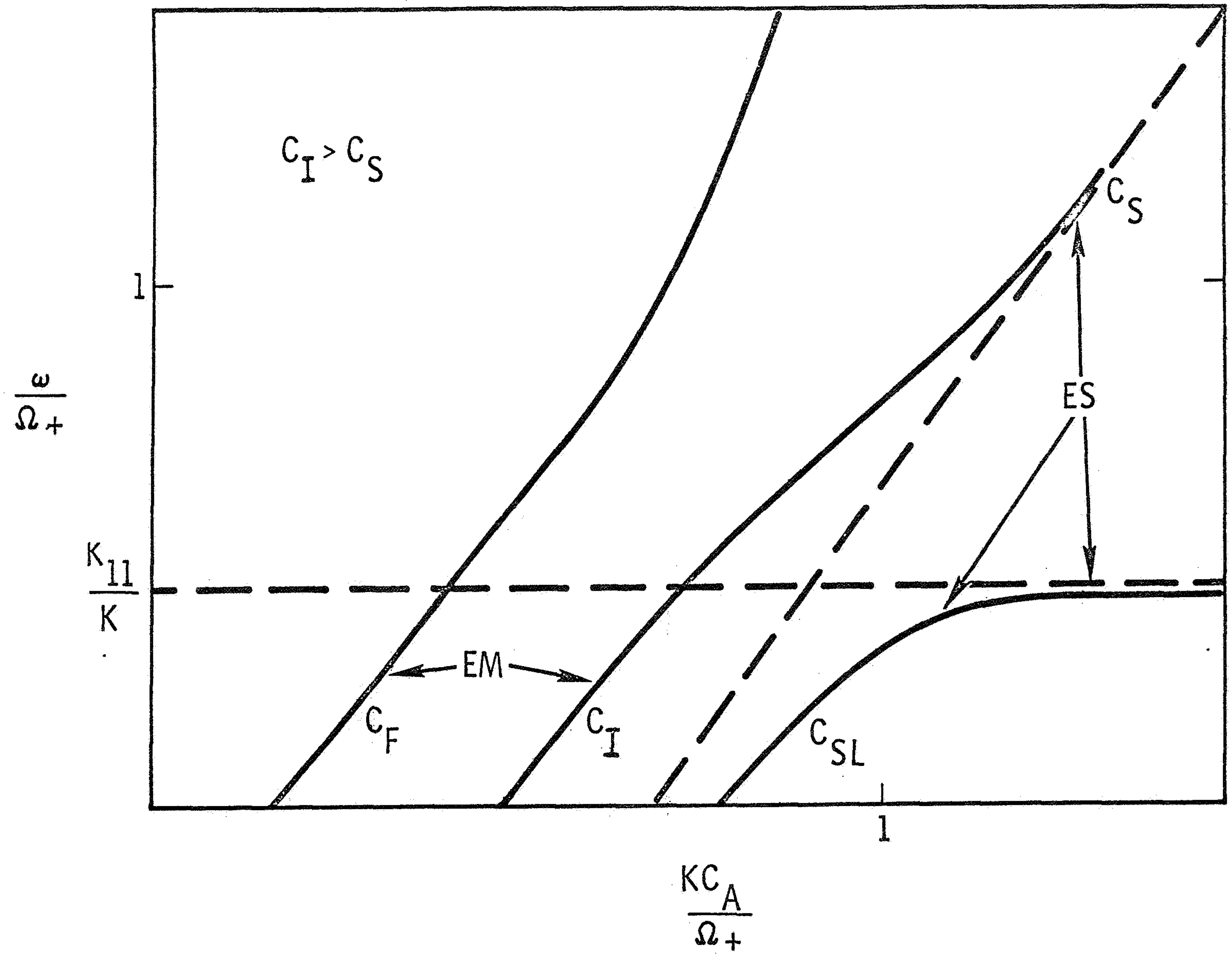

$C_I > C_S$
1
$\frac{\omega}{\Omega_+}$
$\frac{K_{11}}{K}$
C_S
ES
EM
C_F
C_I
C_{SL}
1
$\frac{KC_A}{\Omega_+}$

References

Barcus, J. R., and T. J. Rosenberg, Observations on the spatial structure of pulsating electron precipitation accompanying low frequency hydromagnetic disturbances in the auroral zone, J. Geophys. Res., 70, 1707, 1965.

Barcus, J. R., R. R. Brown, and T. J. Rosenberg, Spatial and temporal character of fast variations in auroral zone x-rays, J. Geophys. Res., 71, 125, 1966.

Braginski, S. I., On the modes of plasma oscillations in a magnetic field, Sov. Phys. Dokl., 2, 345, 1957.

Brice, N. M., Magnetospheric and High Latitude Ionospheric Disturbance Phenomena. In: Physics of the Magnetosphere, R. L. Carovillano, J. F. McCloy, and H. R. Radoski, eds., D. Reidel, Dordrecht, 1968.

Brody, K. I., R. E. Holzer, E. J. Smith, C. F. Kennel, R. W. Fredricks, and F. L. Scarf, Nightside Auroral Electric and Magnetic Noise in the Equatorial Plane, TRANS. Amer. Geophys. Union, 50, 3, 1969.

Coroniti, F. V., and C. F. Kennel, Electron precipitation pulsations, J. Geophys. Res. (this issue).

Cresswell, G. R., and T. N. Davis, Observations on pulsating auroras, J. Geophys. Res., 71, 3155, 1966.

Cummings, W. D., R. J. Sullivan, and P. J. Coleman, Jr., Standing Alfven waves in the magnetosphere, J. Geophys. Res., 74, 778, 1969.

D'Angelo, N., Role of the universal instability in auroral phenomena, J. Geophys. Res., 74, 909, 1969.

Formisano, V. and C. F. Kennel, Small amplitude waves in high β plasmas, J. Plasma Phys., 3, 55, 1969.

Frank, L. A., On the distributions of low energy protons and electrons in the earth's magnetosphere. In: Earth's Particles and Fields, B. M. McCormac, ed., Reinhold Book Corp., N. Y., 1968, p. 67.

Kantrowitz, A. R., and H. E. Petschek, MHD characteristics and shock waves. In: Plasma Physics in Theory and Application, edited by W. B. Kunkel, McGraw Hill Book Co., N. Y., 1966, p. 148.

Kennel, C. F. and J. M. Greene, Finite Larmor radius hydromagnetics, Ann. of Phys., 38, 63, 1966.

Kennel, C. F., Consequences of a magnetospheric plasma, Rev. Geophys., 7, 379, 1969.

Krall, N. A., Drift waves. In: Advances in Plasma Physics, edited by W. B. Thompson and A. Simon, Academic Press, N. Y., 1968.

Liu, C. S., Interchange instabilities of the ring current belt, to be published, J. Geophys. Res., 74, 1969.

McPherron, R. L., G. K. Parks, F. V. Coroniti, and S. H. Ward, Studies of the magnetospheric substorm, 2, Correlated magnetic micropulsations and electron precipitation occurring during auroral substorms, J. Geophys. Res., 1697, 1968.

Mikhailovskii, A. B., and L. I. Rudakov, The stability of a spatially inhomogeneous plasma in a magnetic field, Sov. Phys. JETP, 17, 621, 1963.

Mikhailovskii, A. B., Oscillations of an inhomogeneous plasma. In: Reviews of Plasma Physics, Vol. III, edited by M. A. Leontovich, Consultants Bureau, N. Y., 1967.

Mikhailovskii, A. B., and A. M. Fridman, Drift waves in a finite pressure plasma, Sov. Phys. JETP, 24, 965, 1967.

Parks, G. K., F. V. Coroniti, R. L. McPherron, and K. A. Anderson, Studies of the magnetospheric substorm, 1, Characteristics of modulated electron precipitation occurring during auroral substorms, J. Geophys. Res., 1685, 1968a.

Parks, G. K., T. W. Lezniak, and J. R. Winckler, The Magnetospheric Substorm: A fundamental mode of production of energetic electrons in the outer Van Allen Belt, paper 6-10. International Symposium on the Physics of the Magnetosphere, Washington D. C., Sept. 1968.

Petschek, H. E., and C. F. Kennel, Tail flow, auroral precipitation and ring currents, Trans. Amer. Geophys. Union, 47, 137, 1966.

Rosenbluth, M. N., N. A. Krall, and N. Rostoker, Finite Larmor radius stabilization of weakly unstable confined plasmas, Nuclear Fusion Suppl., pt. 1, 143, 1962.

Rosenbluth, M.N., Microinstabilities. In: Plasma Physics, International Atomic Energy Agency, 1965, p. 485.

Rosenbluth, M. N., Low frequency limit of interchange instability, Phys. Fluids, 11, 869, 1968.

Rukhadze, A. A., and V. P. Silin, Method of geometrical optics in the electrodynamics of an inhomogeneous plasma, Sov. Phys. Uspekhi, 7, 209, 1967.

Rutherford, P. H., and E. A. Frieman, Drift instabilities in general magnetic field configurations, Phys. Fluids, 11, 569, 1968.

Stix, T. H., The Theory of Plasma Waves. McGraw-Hill, N.Y., 1962.

Stringer, T. E., Low frequency waves in an unbounded plasma, Plasma Phys. (J. Nucl. Energy, Part C), 5, 89, 1963.

Swift, D. W., A new interpretation of long period micropulsations, J. Geophys. Res., 72, 4885, 1967.

Vasyliunas, V. M., A survey of low energy electrons in the evening sector of the magnetosphere with OGO 1 and OGO 3, J. Geophys. Res., 73, 2839, 1968a.

Vasyliunas, V. M., Low energy electrons on the day side of the magnetosphere, *J. Geophys. Res.*, *73*, 7519, 1968b.

Wilson, C. R., Conjugate three dimensional polarization of high latitude micropulsations from a hydromagnetic wave-ionospheric current model, *J. Geophys. Res.*, *71*, 3233, 1966.